P_- which interact with each other and transmit traction.

For a given plane P, (i) we can take the set P_+ as that fixed set of atoms whose long-time average positions lie on the positive side of **n**, and similarly for P_-, or (ii) we can take the set P_+ as the variable set of atoms which at a given instant lie on the positive side of **n**. We refer to (i) as the material description and to (ii) as the spatial description. We employed the material descriptions in ref 11 and 12 and have employed both here. It is important to note that the momentum transfer across the fixed plane must be included when the spatial description is employed.

In the present paper we have focused on the nature of the generalized virial stress formula and the insights it provides into the character of stress and traction in a rubberlike material. In the following paper we will use this formula as a means for studying the validity of the ideal chain assumption in rubber elasticity.

References and Notes

(1) This paper is based on the research of J. Gao performed in partial fulfillment of the requirements for the Ph.D. in Physics at Brown University. This work has been supported by the Gas Research Institute (Contract 5085-260-1152), by the National Science Foundation through the Materials Research Laboratory, Brown University, and by the National Science Foundation, Polymers Program, which provided computer time at the supercomputer centers at the University of Minnesota and at the University of Illinois.
(2) A more extended discussion of excluded volume is contained in: Gao, J.; Weiner, J. H. *Macromolecules*, following paper in this issue.
(3) Swenson, R. J. *Am. J. Phys.* **1983**, *51*, 940.
(4) Ray, J. R.; Moody, M. C.; Rahman, A. *Phys. Rev. B* **1985**, *32*, 733.
(5) Theodorou, D. N.; Suter, U. W. *Macromolecules* **1986**, *19*, 139.
(6) Kluge, M. D.; Ray, J. R.; Rahman, A. *J. Chem. Phys.* **1986**, *85*, 4028.
(7) See, for example: Ogden, R. W. *Rubber Chem. Technol.* **1986**, *59*, 361.
(8) Weiner, J. H. *J. Chem. Phys.* **1986**, *85*, 2910.
(9) Weiner, J. H. *Statistical Mechanics of Elasticity*; Wiley: New York, 1983.
(10) Weiner, J. H.; Berman, D. H. *J. Polym. Sci., Polym. Phys. Ed.* **1986**, *24*, 389.
(11) Gao, J.; Weiner, J. H. *Macromolecules* **1987**, *20*, 142.
(12) Gao, J.; Weiner, J. H. *J. Chem. Phys.* **1984**, *81*, 6176.

Excluded-Volume Effects in Rubber Elasticity. 2. Ideal Chain Assumption[1]

J. Gao and J. H. Weiner*

Department of Physics and Division of Engineering, Brown University, Providence, Rhode Island 02912.

Received March 12, 1987; Revised Manuscript Received June 10, 1987

ABSTRACT: A key assumption in most theories of rubber elasticity is that the network can be regarded as a system of noninteracting ideal chains. Excluded-volume effects enter only as the agency responsible for maintaining the material at constant volume. As a test of this approach, molecular dynamics calculations are performed for a three-chain model using freely jointed chains and a truncated Lennard-Jones approximation to hard-sphere excluded volume. The state of stress in this model when subjected to constant volume uniaxial extension is determined from the molecular dynamics calculations by use of the virial stress formula and compared with the stress predicted on the basis of the ideal chain assumption. Significant, density-dependent differences are found. Molecular dynamics calculations for a polymer melt show that the force–length relation for a chain in the melt approaches the ideal relation as the melt density is increased, in accord with the Flory theorem, but they also show that this is due to large intermolecular noncovalent contributions to the force. Since noncovalent interactions do not contribute to the deviatoric stress in the model studied, the observed nonideal behavior is not inconsistent with the Flory theorem.

Introduction

The concept of an ideal chain,[2] which occupies a central position in polymer physics, may be described as follows. The covalent bonds between the backbone atoms and side groups of a linear macromolecule are primarily responsible for its characteristic behavior. There are, in addition, noncovalent interactions; these act between atoms which are neighboring along the chain (i.e., nearby side–group interactions) as well as between atoms which are widely separated along the chain but happen to be in close proximity because of the chain's long-range flexibility. A linear chain model which may include the former noncovalent interactions but omits the latter is said to be ideal. In particular, an ideal chain model omits the repulsive excluded-volume interaction which prevents the chain from doubling back on itself and causing two atoms, widely separated along the chain, to occupy the same place in space.

Ideal chain models exhibit some universal characteristics that are independent of the local chain structure, i.e., of bond angle restrictions and local noncovalent interactions. For example the probability density $p(\mathbf{R})$ for an end-to-end displacement **R** becomes Gaussian as N, the number of bonds, becomes sufficiently large and $\langle R^2 \rangle \sim N$. In contrast, for an isolated chain model with excluded volume interactions, $\langle R^2 \rangle \sim N^{1.2}$, and the latter prediction has been well confirmed by experiment for linear macromolecules in dilute solution.

For a dense uncross-linked system of like molecules, a polymer melt, Flory[3] has predicted that the excluded-volume potential for any given molecule would be screened by the others and that $p(\mathbf{R})$ for an individual molecule would be ideal. This remarkable result, sometimes termed[2] the Flory theorem, has been confirmed experimentally[4] and by computer simulation[5] as far as the scaling behavior of $\langle R^2 \rangle$ is concerned.

In the subject of rubber elasticity we are concerned with the mechanical behavior of a cross-linked amorphous network of long-chain molecules. The long-time behavior of the end-to-end displacement vector **R** of a particular chain of the system provides an important distinction between a melt, in which $\langle \mathbf{R} \rangle = \mathbf{0}$, and a network in which

0024-9297/87/2220-2525$01.50/0

$\langle \mathbf{R} \rangle \neq \mathbf{0}$.[7] The basic molecular theory of rubber elasticity was begun over 50 years ago and remains an active subject of research.[8] While many aspects of the theory, such as the role of network connectivity,[9] nature of cross-link fluctuation dependence on deformation,[9-11] and effect of finite chains,[12] are under investigation, we are here concerned with the role of excluded volume. In most treatments of the subject, the network is regarded as a collection of ideal, noninteracting chains (sometimes referred to as a phantom network[9]). Excluded-volume interactions are frequently incorporated only through the statement (sometimes tacit) that they are the agency responsible for maintaining the system at a constant volume. With this latter assumption, as discussed in ref 13, hereafter referred to as paper 1, the mean or hydrostatic stress is not determined from the constitutive relation but from the imposed stress boundary conditions.

Another approach[14] that has been employed to treat excluded-volume effects is to postulate that the Helmholtz free energy of the system $F(\lambda_1,\lambda_2,\lambda_3,T)$, for stretch ratios λ_j, $j = 1, 2, 3$, and temperature T, can be written as a sum

$$F(\lambda_1,\lambda_2,\lambda_3,T) = F_C(\lambda_1,\lambda_2,\lambda_3,T) + F_E(v,T)$$

where F_C is the free energy of the collection of ideal chains, v is the present volume of the system, and F_E is due to excluded-volume interactions. The quantity $\partial F_E/\partial v$ plays the role of the mean stress[15] and is again determined from the imposed boundary conditions.

Studies directed toward the justification of this type of decomposition on the basis of atomic theories have been presented by Boggs[16] and Eichinger.[17] Other treatments of excluded-volume effects have been given by DiMarzio,[18] Jackson, Shen, and McQuarrie,[19] and Gaylord.[20] These works all take as their starting point the chain view of stress in the terminology of paper 1. In the present paper we examine excluded-volume effects in rubber elasticity on the basis of computer simulation of an idealized network model and gain a different view of the phenomenon by using the virial stress formula discussed in paper 1 to interpret the results.

We begin in section 1 with the computer simulation by molecular dynamics of a polymer melt of a system of freely jointed chains with a truncated Lennard-Jones approximation to hard-sphere interactions, i.e., the same model treated in paper 1. Whereas earlier computer simulation tests of the Flory theorem had been confined to checking the predictions regarding $\langle R^2 \rangle$ (and in the case of ref 6, of $\langle R^4 \rangle$), in these calculations the full probability density distribution, $p(\mathbf{R})$, is evaluated. This then permits the calculation of the axial force f dependence on R for the strain ensemble; these results are in accord with the Flory theorem in that the calculated $f(R)$ relation approaches that of the ideal chain as the melt density is increased.

We then turn in section 2 to the computer simulation by molecular dynamics of a simple network of the same model chains. The network corresponds to the familiar three-chain model of rubber elasticity so that it is straightforward to compute the stress corresponding to a given uniaxial extension under the assumption that the chains are ideal and noninteracting. The exact stress is found by application of the virial formula discussed in paper 1, and it is found that, in general, the two values of the stress do not agree.

In an attempt to reconcile the results for the melt and for the network, we return in section 3 to the former and compute by molecular dynamics a decomposition of the axial force f for fixed $\mathbf{R}$ into its covalent f_c and noncovalent f_{nc} contributions. The manner of the relative variation of f_c and f_{nc} with melt density suggests a basis for the breakdown of the ideal chain assumption for the three-chain model of section 2. Finally, a summary and further conclusions are presented in section 4.

1. Polymer Melt Simulation

We treat the freely jointed, hard-sphere model described in section 1 of paper 1 and consider a melt consisting of ν identical molecules with N bonds each in a cubic cell of side L_0 and with periodic boundary conditions. The reduced atom number density of the system, ρ, is then defined as

$$\rho = \nu(N + 1)\sigma^3/L_0^3 \tag{1.1}$$

where σ is the hard-sphere diameter. (All atoms of the system interact with this hard-sphere potential.) The motion of the system is determined by the molecular dynamics procedure described in the Appendix. The program includes a sorting routine on R, the fluctuating end-to-end distance of all the molecules, and this leads to a numerical estimate for the probability density $P(R)$ from which we may then obtain $p(\mathbf{R})$ by the relation $4\pi R^2 p(\mathbf{R}) = P(R)$.

We now assume that a particular molecule of the system has its end-to-end displacement, $\mathbf{x}_N - \mathbf{x}_0$, fixed at a particular value $\mathbf{R}$ while the remaining molecules move freely as before. Then the potential energy, $V(\mathbf{x}_0,...,\mathbf{x}_N;\mathbf{R})$, of the selected molecule can be written as $V = V_{int} + V_{eff}$, where $V_{int}(\mathbf{x}_0,...,\mathbf{x}_N)$ is the intramolecular potential energy and $V_{eff}(\mathbf{x}_0,...,\mathbf{x}_N;\mathbf{R})$ is the effective mean-field potential of interaction of the atoms of the fixed molecule with the remaining molecules of the melt. Then, as is the case for a single isolated molecule, we can show[21] that $p(\mathbf{R}) = CZ(\mathbf{R},T)$ where $Z(\mathbf{R},T)$ is the configurational partition function for the fixed molecule in the strain ensemble (that is, for fixed end-to-end displacement $\mathbf{R}$) and C is $\mathbf{R}$ independent. It then follows in the usual way[21] that the axial force f required to maintain the end-to-end distance R for a single molecule surrounded by the melt is

$$f = -kT\frac{\partial}{\partial R} \ln p(\mathbf{R}) \tag{1.2}$$

so that the $f(R)$ relation for molecules in the strain ensemble for melts of different densities may be obtained by numerical differentiation of $p(\mathbf{R})$. An example of the direct result of numerical differentiation is shown in Figure 1 which indicates the scatter inherent in this process; also shown is a cubic spline fit used to smooth the numerical results. All of the model parameters used in this paper have the same values as in paper 1 except here $\kappa a^2/kT = 2024$.

Results of this procedure for various densities are shown in Figure 2. Although the numerical procedure leads to some inaccuracies and irregularities, the trend with density is clear. At very low density, the $f(R)$ relation shows the same general character as found previously[22] for chain models with excluded volume in the strain ensemble; most importantly, the relation exhibits a compressive regime ($f < 0$) for sufficiently small R. As the density ρ increases, this compressive regime disappears and the $f(R)$ relation approaches that of the ideal chain ($\sigma = 0$). Although it was not possible, because of computer time restrictions, to simulate the high values of ρ sufficient for complete convergence, the results appear to be in good accord with the Flory theorem.

2. Three-Chain Model

We consider next a system which models a cross-linked network of the freely jointed, hard-sphere chains. The system is based on the familiar three-chain model of rubber

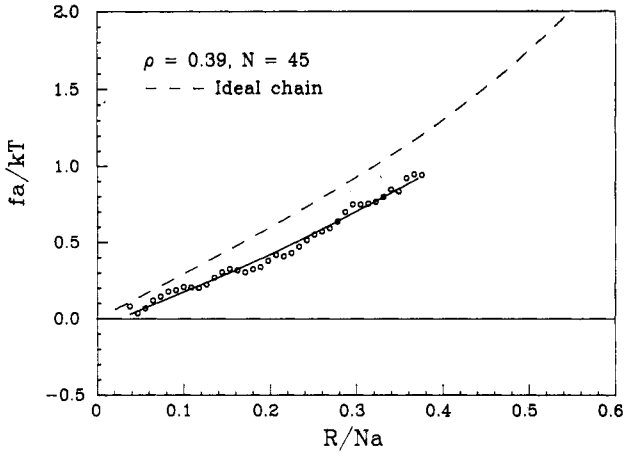

Figure 1. Force–length relation for a chain in a melt as obtained by use of eq 1.2 from molecular dynamics simulation with intra- and intermolecular excluded-volume interactions. Points are the direct results of numerical differentiation; the solid curve is a cubic spline fit. The dashed curve is the corresponding relation for an ideal chain.

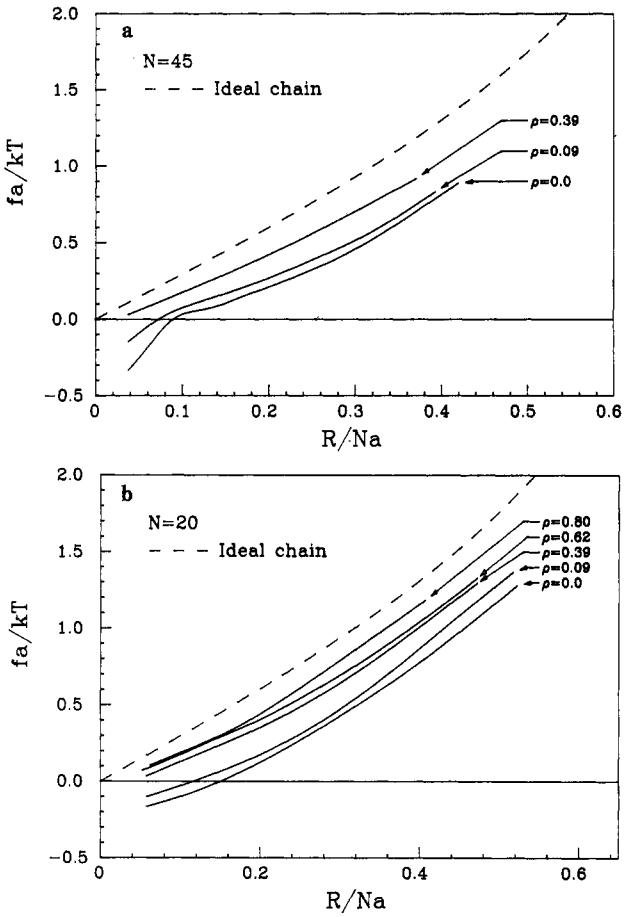

Figure 2. Force–length relations obtained by a cubic spline fit to results of numerical differentiation as described in caption to Figure 1, for various melt densities. The curve for $\rho = 0$ corresponds to single chain with no surrounding melt. (a) $N = 45$: for $\rho = 0.09$, eq 1.1, $\nu = 6$ and $L_0 = 11.6a$; for $\rho = 0.39$, $\nu = 6$ and $L_0 = 7.1a$. (b) $N = 20$: for $\rho = 0.09$, $\nu = 10$ and $L_0 = 10.6a$; for $\rho = 0.39$, $\nu = 10$ and $L_0 = 6.5a$; for $\rho = 0.62$, $\nu = 15$ and $L_0 = 6.4a$; for $\rho = 0.80$, $\nu = 15$ and $L_0 = 5.9a$.

elasticity.[23] To construct the system in the reference state, we start with a cube of side L_0 centered at the origin of a rectangular Cartesian coordinate system. A total of ν chains, each with N bonds, are located in the cube, with $\nu/3$ chains running in each coordinate direction with their end atoms fixed in the cube planes perpendicular to that direction. (Care was taken in the generation of the initial chain configurations to avoid any topological entanglements. For the parameters employed here for the covalent and noncovalent potentials a minimum energy of $\sim 40kT$ would be required for one chain to pass through another; the initial topology is therefore conserved to very high probability.) Periodic boundary conditions are employed in all three coordinate directions, and the fixed end points are located so that chain density is uniform in space. The system is subjected to a uniaxial deformation at constant volume so that the cube side in the x_1 direction has length λL_0 while the other two sides have length $\lambda^{-1/2}L_0$.

In what follows we take the atom number density ρ, eq 1.1, as an independent parameter, with the variation in behavior of the system with ρ as a question of particular interest. Neither in the reference or deformed state do we regard the pressure p which corresponds to a particular value of ρ as physically significant, since the hard-sphere potential of the model lacks an attractive tail. Therefore, we focus upon the deviatoric stress,[13] τ_{11}, and its variation with λ. This viewpoint is in accord with that in the modern theory of liquids, termed the van der Waals picture,[24] in which the role of the strong short-ranged repulsive force is emphasized. To quote from ref 24, "Attractive forces...play a minor role in the structure, and in the simplest approximation their effect can be treated in terms of a mean field—a spatially uniform background potential—which...merely provides the cohesive energy that makes the system stable at a particular density and pressure."

Noninteracting Chains. If we make the usual assumption that the chains are noninteracting then it is straightforward to obtain the $\tau_{11}(\lambda)$ relation. Let $\hat{F}(R)$ be the Helmholtz free energy per chain so that

$$f(R) = \frac{\partial \hat{F}(R)}{\partial R} = \hat{F}'(R) \tag{2.1}$$

is its force–length relation. Then the total free energy F per unit volume of the system is

$$F = \frac{\nu}{3L_0^3}(\hat{F}(\lambda_1 L_0) + \hat{F}(\lambda_2 L_0) + \hat{F}(\lambda_3 L_0)) \tag{2.2}$$

where, for uniaxial extension at constant volume, $\lambda_1 = \lambda$, $\lambda_2 = \lambda_3 = \lambda^{-1/2}$. Application of eq 1.11 of paper 1, together with eq 2.1, then leads to

$$\tau_{11} = \frac{2\nu}{9L_0^2}(\lambda f(\lambda L_0) - \lambda^{-1/2} f(\lambda^{-1/2} L_0)) \tag{2.3}$$

If the system has lateral faces free of stress, $t_{22} = t_{33} = 0$, then (eq 1.9 of paper 1) $p = -{}^1/_3 t_{11}$ and (eq 1.8 of paper 1) $\tau_{11} = {}^2/_3 t_{11}$ and it is seen that eq 2.3 is equivalent to the familiar result for the three-chain model.[23] If the chains are taken as ideal, then $p(\mathbf{R})$ is given by the Treloar formula[25] for freely jointed ideal chains and $f(R)$ is determined from eq 1.2.

Computer Simulation of the Model. Computer simulation of the model with full atom interactions (inter- and intrachain and between principal and image atoms) included is carried out by molecular dynamics and the values of τ_{11} computed by means of the virial stress formula, eq 1.13 of paper 1. Details of the numerical procedure are contained in the Appendix.

Results of these computer simulations for $\tau_{11}(\lambda)$ for four different values of ρ are shown in Figure 3, together with the theoretical result, eq 2.3, based on noninteracting ideal chains. It is seen that ρ has a systematic effect on the nature of the $\tau_{11}(\lambda)$ dependence, and only for a single value of ρ, $\rho = 0.092$, do the two results coincide.

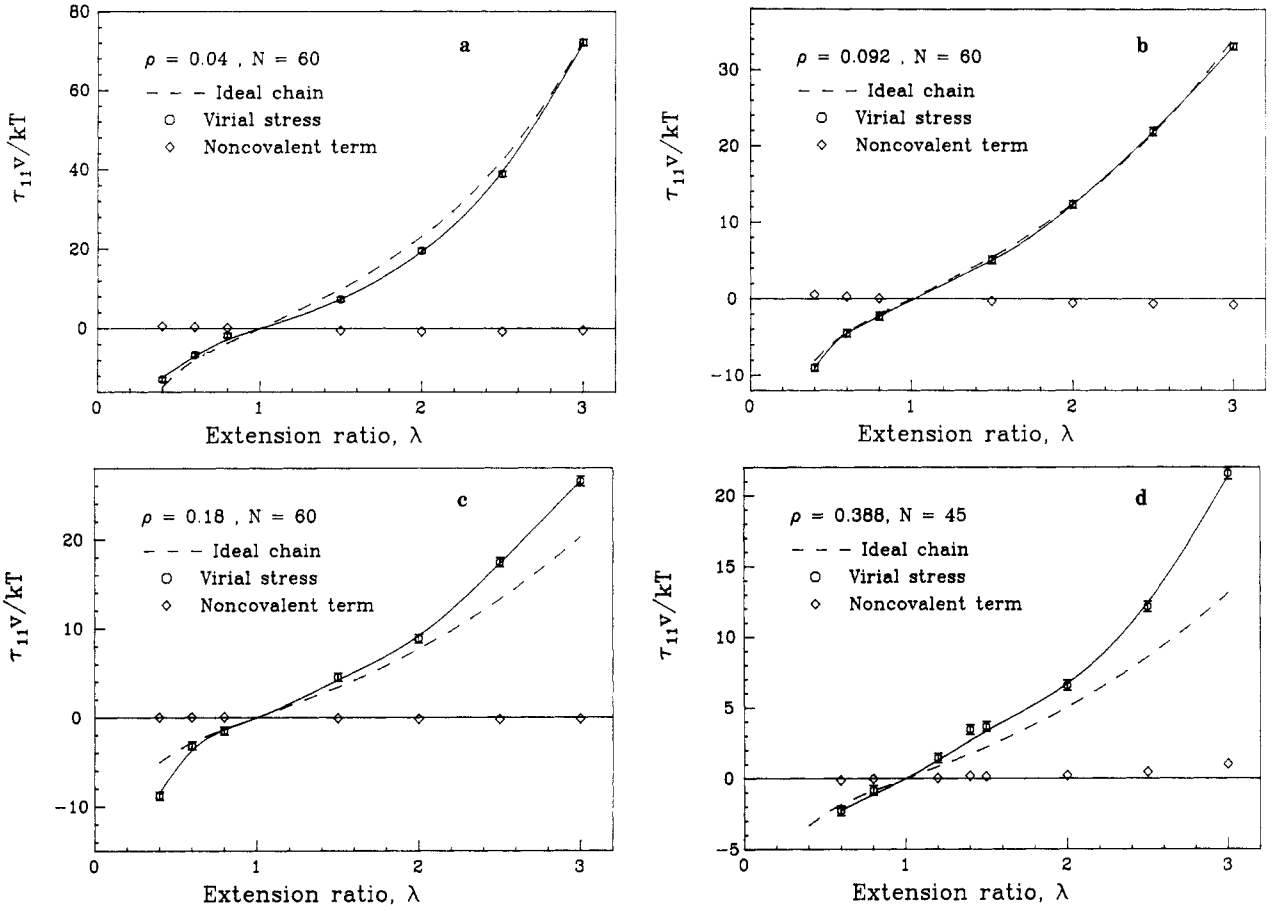

Figure 3. Deviatoric stress τ_{11} in three-chain model with intra- and interchain excluded volume interactions, as computed from molecular dynamics simulation on the basis of the virial stress formula, eq 2.4–2.6. The solid curve is a cubic spline fit through computer points; error bar computed as described in Appendix. Points shown by diamonds represent the noncovalent contribution, τ_{11}^{nc}, as defined in eq 2.6. Shown for comparison (as dashed curve) is the result of use of the ideal chain relation in the conventional three-chain formula, eq 2.3: (a) $\rho = 0.04$, $L_0/N_a = 0.220$; (b) $\rho = 0.092$, $L_0/Na = 0.167$; (c) $\rho = 0.18$, $L_0/Na = 0.133$; (d) $\rho = 0.388$, $L_0/Na = 0.125$.

In an attempt to gain insight into the cause of the discrepancy we write

$$\tau_{11} = \tau_{11}^{c} + \tau_{11}^{nc} \tag{2.4}$$

where, from the virial stress formula (eq 1.13 of paper 1),

$$\tau_{11}^{c} = (1/3v) \sum_{\alpha \in c} \langle r_\alpha u'_c(r_\alpha)[3 \cos^2 \theta_\alpha - 1] \rangle \tag{2.5}$$

$$\tau_{11}^{nc} = (1/3v) \sum_{\alpha \in nc} \langle r_\alpha u'_{nc}(r_\alpha)[3 \cos^2 \theta_\alpha - 1] \rangle \tag{2.6}$$

where θ_α is the angle made by $\mathbf{r}_\alpha$ with the x_1 axis, and we recall that $\mathbf{r}_\alpha$ represents a covalent bond for $\alpha \in$ c and the vector connecting an arbitrary pair of atoms in noncovalent interaction for $\alpha \in$ nc. The numerical results (Figure 3) show that τ_{11}^{nc} remains very small for all values of λ; i.e., the direct contribution of the noncovalent potential to the stress tensor, for the present hard-sphere model, is essentially hydrostatic.

However, it is clear that the noncovalent potential makes an important indirect contribution by affecting τ_{11}^{c}, for if the latter were unchanged we would have agreement with ideal chain behavior at all ρ. We may gain additional insight into the way the noncovalent potential affects τ_{11}^{c} by examining the average bond force f_b. The calculation of this quantity is included as part of the three-chain model program; it is averaged separately for each of the chains so that its value is obtained as a function of R/Na as well as of ρ. The effect of excluded volume on the bond force has also been computed by molecular dynamics simulation of a single chain so that only intrachain noncovalent effects are present. The results of these calculations are shown in Figure 4, together with the theoretical variation of an ideal chain.[26] It is seen that excluded volume has a significant effect upon the bond force and furthermore this effect is density dependent.

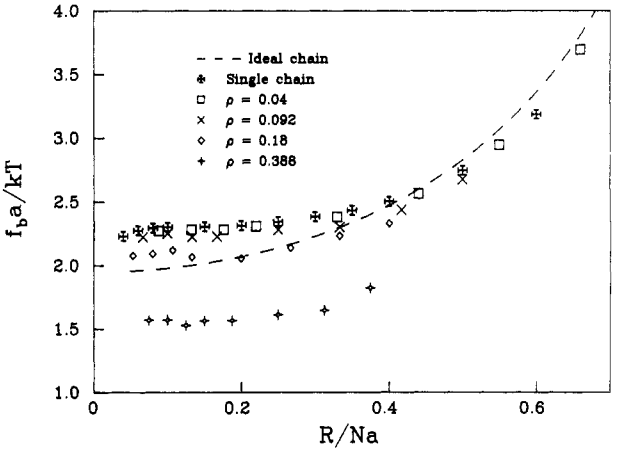

Figure 4. Effect of excluded volume on average bond force, f_b, as determined from molecular dynamic simulation of a single chain as described in paper 1, Section 3, and, for various values of density ρ, of a three-chain model. All computations are for $N = 60$ with the exception of that for $\rho = 0.388$ for which $N = 45$. The ideal chain result is based on theory[26] and is evaluated for $N = 60$; the theoretical result for $N = 45$ is very close in value.

3. Polymer Melt: Direct Force Calculation

In section 1, the force–length relation for a long-chain molecule in a melt was computed by means of a molecular dynamics simulation in which all molecules are free. This simulation yields the probability density $p(\mathbf{R})$ for the

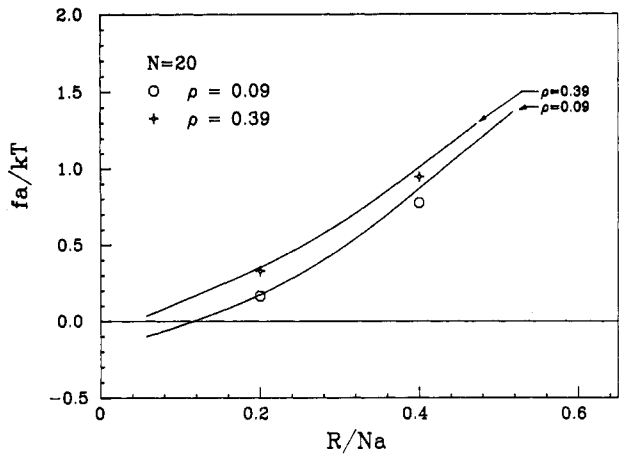

Figure 5. Comparison of the axial force f on a single chain with fixed end-to-end distance surrounded by the melt as computed by eq 1.2, solid curves, and as computed by direct calculation at $R/Na = 0.2$ and 0.4 for melt densities $\rho = 0.09$ and 0.39. Values of ν and L_0 are as in Figure 2 for corresponding densities.

end-to-end displacement **R** and the $f(R)$ relation is then determined from eq 1.2.

To gain further insight, in this section we consider a molecular dynamics simulation which leads to a direct calculation of the force. That is, we select one molecule of the melt and fix both of its end atoms with a prescribed end-to-end displacement **R**. The other molecules of the melt remain free to move and the time averages of the resultant of all forces (inter- and intramolecular) on the fixed end atoms are computed directly. Taking into consideration statistical fluctuations in the calculations, it is seen from Figure 5 that the two methods are in reasonably good agreement.

The direct method of computation clearly requires substantially more computer time than the indirect method of section 1 which gave the entire $f(R)$ relation from a single simulation; it is for this reason that the value of f is computed for only two values of R by the direct method. The advantage of the direct method, however, is that it allows a detailed decomposition of the force acting on the end atoms into its covalent and noncovalent parts and a further decomposition of the latter into its intra- and its intermolecular portions.

Let $\mathbf{x}_0$ and $\mathbf{x}_N$ be the fixed end atoms, and $\mathbf{R} = \mathbf{x}_N - \mathbf{x}_0 = R\mathbf{e}$. The program computes separately the following parts of the force acting on atom N of the fixed molecule: (a) $\mathbf{g}_c$, the covalent force transmitted through the bond between atoms $N-1$ and N; (b) $\mathbf{g}_{intra}$, the noncovalent force exerted by atoms 1, ..., $N-1$ of the fixed molecule; (c) $\mathbf{g}_{inter}$, the noncovalent force exerted by the other molecules of the melt.

In order that it be held fixed, atom N must be subjected to an external force $\mathbf{f} = -(\mathbf{g}_c + \mathbf{g}_{intra} + \mathbf{g}_{inter})$ and it is convenient to introduce the notation

$$f_c = -\langle \mathbf{g}_c \cdot \mathbf{e} \rangle \qquad f_{intra} = -\langle \mathbf{g}_{intra} \cdot \mathbf{e} \rangle$$
$$f_{inter} = -\langle \mathbf{g}_{inter} \cdot \mathbf{e} \rangle \tag{3.1}$$

where, it is seen, f_c is the time average of the axial component of that portion of the external force f required to balance the covalent force exerted on atom N, and similarly for f_{intra} and f_{inter}.

From their manner of definition, it is seen that $f_c > 0$ corresponds to a required tensile force and $f_c < 0$ to a required compressive force, and similarly for f_{intra} and f_{inter}. In our previous studies on an isolated chain, we have seen that $f_c > 0$ and f_{nc} ($=f_{intra}$) < 0. Results for the chain in the melt are shown in Figure 6; as seen there, $f_{intra} < 0$ as

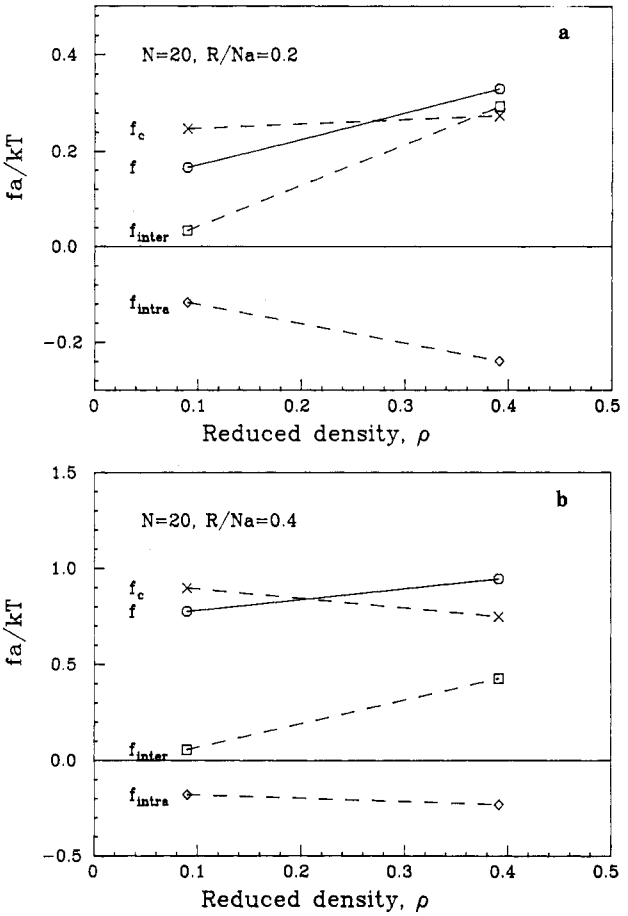

Figure 6. Decomposition of axial force f on a chain in the melt, with fixed end-to-end distance R, into the sum $f = f_c + f_{intra} + f_{inter}$, where f_c is due to the covalent bonds of the molecule, f_{intra} is the intramolecular noncovalent contribution, and f_{inter} is the intermolecular noncovalent contribution: (a) $R/Na = 0.2$; (b) $R/Na = 0.4$.

in the isolated chain, but $f_{inter} > 0$. The latter result may be understood as follows: if atom N were an isolated atom in the melt (i.e., if there were no chain attached to it) then it is clear that $\langle \mathbf{g}_{inter} \rangle = 0$ since all directions of interactions would be equally likely. However, the presence of the chain with fixed $\mathbf{x}_N - \mathbf{x}_0 = R\mathbf{e}$, preferentially screens atom N from hard-sphere interaction with atoms of the melt that lie in the $-\mathbf{e}$ direction. Therefore $\langle \mathbf{g}_{inter} \cdot \mathbf{e} \rangle < 0$ and, from eq 3.1, $f_{inter} > 0$.

As seen in section 1, an increase in ρ, the melt density, causes the $f(R)$ relation for a chain in the melt to increase toward the ideal chain relation in accord with the Flory theorem. The present decomposition shows that this increase is primarily due to the intermolecular noncovalent interaction. This is seen in Figure 6 for both $R/Na = 0.2$ and 0.4; for the latter value, for example, f_c decreases with ρ, f_{intra} remains nearly constant, and it is only the increase in f_{inter} that is responsible for the increase in f with ρ.

4. Conclusions

Our computer simulations of freely jointed, hard-sphere chains have shown that the axial force f required to maintain a fixed end-to-end distance R approaches ideal behavior, i.e., that predicted in the absence of excluded volume, when the given chain is surrounded by a high-density melt of similar chains. This is in accord with the Flory theorem.

At the same time, computer simulation of a network of such chains, corresponding to the three-chain model of rubber elasticity, shows that the usual assumption of treating the chains as ideal and noninteracting leads to

values of the stress which are in disagreement with those determined from the molecular dynamics results on the basis of the virial stress formula.

This difference in behavior between the melt and the network may be reconciled as follows: The usual isochoric assumption of rubber elasticity leaves the pressure or mean stress to be determined by the stress boundary conditions and only the deviatoric stress to be determined by the constitutive relations.[13] As observed in the computer simulation of the network, the noncovalent excluded volume interactions contribute only to the hydrostatic portion of the stress and make negligible contribution to the deviatoric stress. Equivalently, the deviatoric stress in the network is determined solely by the covalent potential. For the chain in the melt, we have seen that the approach to ideal behavior of the $f(R)$ relation is achieved only because of the density dependence of the intermolecular noncovalent contribution; the covalent contribution remains far from ideal. In fact, the significant excluded volume effect upon the covalent interactions is seen most clearly in the behavior of the bond forces, Figure 4. Therefore, in the network, where the deviatoric stress is determined almost solely by the covalent forces, nonideal behavior is observed.

While the model studied in this paper is too idealized to permit us to draw direct conclusions about real materials, these simulations do provide insights and caveats which should be applicable. In recent years there have been a number of experimental investigations directed toward testing the ideal chain assumption in networks. They have attempted, with the use of neutron scattering techniques, to probe the distribution of configurations of marked chains. The premise on which these tests rests is that the observation of an ideal distribution for such a chain would verify the procedure of computing stress on the assumption of a noninteracting collection of ideal chains.[9]

The results of the present computer simulations show that this reasoning need not be valid. The ideal distribution may come about as a consequence of noncovalent interactions which do not, however, contribute significantly to the deviatoric stress. Furthermore, the covalent interactions which do contribute directly to this stress may be far from ideal as a consequence of the excluded-volume effect.

Appendix: Molecular Dynamics Procedure

The molecular dynamics procedure used is similar to that described previously in ref 27. A calculation of the time evolution of the system corresponding to given initial positions and velocities is performed, using the Verlet algorithm, for a period of time referred to as a block. A new set of initial velocities is then chosen, corresponding to a canonical ensemble at the prescribed temperature, and the process is repeated. A typical computation used 400 blocks, each with 5000 time steps. A time step $\Delta t = 0.1$ was used in units of $(m/\kappa)^{1/2}$. For a carbon–carbon bond this corresponds to $\Delta t = 7.7 \times 10^{-16}$ s.

The computer program employed nearest-neighbor tables with the most time consuming subroutines designed to be vectorizable by the Cray Fortran compiler.[28] The usual way to impose periodic boundary conditions is to exchange the real atoms and their images when they cross the boundaries of a periodic cell. The real atoms refer to those within the principal cell and are explicitly simulated. Dealing only with the real atoms makes the noncovalent force computation simpler and easily vectorized. The covalent bonds require different treatment. Since they cannot be broken during the simulation, the programs store the information as to which covalent bonds exist between atom pairs with at least one atom of the pair being a real atom. This is done by an array that indicates which atoms should be replaced by their images before the covalent forces between these pairs of atoms are computed. The values of this array are updated periodically. With the help of this array the computation of the covalent forces is still vectorizable and runs efficiently. This array was also useful in the computation of average atom positions.

In order to compute the transmitted forces through a material plane in the single-chain simulation, we used a different method for imposing the periodic boundary condition. The atoms on the principal chain are always real atoms. However, in order to determine the noncovalent portion of transmitted forces through any material plane, noncovalent forces have to be computed between all possible pairs of atoms, real and imaginary. This scheme is difficult to apply to a multichain system with periodic boundary conditions in three perpendicular directions. In this case the force decomposition is made by computing the covalent part of transmitted force through any material plane and using the virial stress formula to find the total transmitted force; the noncovalent part is then obtained by subtraction.

The initial configurations were generated in the following way: A backbone structure is created by a forced random walk with $\sigma = 0$; then σ is allowed to grow during the first stage of simulation until it reaches the given value. The computation is then continued for an incubation period in order to release or absorb the extra energy so that it has the correct internal energy at the beginning of the accumulation of data. Care was taken in the generation of the initial configurations of the three-chain system to ensure that no entanglements were present.

In order, in paper 1, to get uniform results for a single chain within reasonable computer time, we used the smaller value of $\kappa a^2/kT = 202$. As indicated in Section 1 of paper 1, this caused some deviation in the axial force f for the computed ideal chain from the theoretical results for the large κ limit, but this deviation was significant only at a large extension of the chain, e.g., $r/Na > 0.7$. The value of $\kappa a^2/kT = 2024$ used in this paper provided results much closer to those of the large κ limit but produced greater scatter for a given computation period.

Another technical problem is that in multichain simulation, the noncovalent interactions between a chain and its image are counted as intrachain noncovalent interactions for programming convenience. However, these interactions are believed to be very small and will therefore not affect the interchain and intrachain decomposition of the noncovalent contribution.

The computer time is strongly dependent on the number density. On the CRAY X-MP, a typical result for a system containing three 60-bond chains at number density $\rho = 0.18$ requires approximately 3900 s of cpu time for 2×10^6 time steps.

Error bars for τ_{11} shown in Figure 3 of extent $\pm\sigma$ were computed by treating the value $\tau_b = \langle\tau_{11}\rangle_b$ determined by averaging over each of the M blocks of the molecular dynamics calculation as an independent determination and then computing $\sigma = [\sum_b(\Delta\tau_b)^2]^{1/2}/M$.

References and Notes

(1) This paper is based on the research of J. Gao performed in partial fulfillment of the requirements for the Ph.D. in Physics at Brown University. This work has been supported by the Gas Research Institute (Contract 5085-260-1152), by the National Science Foundation through the Materials Research Laboratory, Brown University, and by the National Science

Foundation, Polymers Program, which provided computer time at the supercomputer centers at the University of Minnesota and at the University of Illinois.

(2) de Gennes, P.-G. *Scaling Concepts in Polymer Physics*; Cornell University: Ithaca, NY, 1979.
(3) Flory, P. J. *J. Chem. Phys.* **1949**, *17*, 303.
(4) Daoud, M.; Cotton, J. P.; Farnoux, B.; Jannink, G.; Sarma, G.; Benoit, H.; Duzlessix, R.; Picot, C.; de Gennes, P.-G. *Macromolecules* **1975**, *8*, 804.
(5) Curro, J. G. *J. Chem. Phys.* **1974**, *61*, 1203. Khalatur, P. G.; Papulov, Yu. G.; Pavlov, A. S. *Mol. Phys.* **1986**, *58*, 887.
(6) Curro, J. G. *Macromolecules* **1979**, *12*, 463.
(7) Ullman, R. *Macromolecules* **1986**, *19*, 1748. Our notation differs from this reference in that brackets denote long-time averages for a single chain.
(8) For historical and general presentations of the theory, see: Flory, P. J. *Theory of Polymer Chemistry*; Cornell University: Ithaca, NY, 1953. Treloar, L. R. G. *The Physics of Rubber Elasticity*, 3rd ed.; Clarendon: Oxford, 1975. Recent reviews are given by: Eichinger, B. E. *Annu. Rev. Phys. Chem.* **1983**, *34*, 359. Ullman, R. *J. Polym. Sci., Polym. Symp.* **1985**, *72*, 39.
(9) Flory, P. J. *Proc. R. Soc. London, A* **1976**, *351*, 351.
(10) Ronca, G.; Allegra, G. *J. Chem. Phys.* **1975**, *63*, 4990.
(11) Flory, P. J.; Erman, B. *Macromolecules* **1982**, *15*, 800.
(12) Mark, J. E.; Curro, J. G. *J. Chem. Phys.* **1983**, *79*, 5705.
(13) Gao, J.; Weiner, J. H. *Macromolecules*, preceding paper in this issue.
(14) James, H. M.; Guth, E. *J. Polym. Sci.* **1949**, *4*, 153.
(15) In an earlier paper (Gao, J.; Weiner, J. H. *J. Chem. Phys.* **1984**, *81*, 6176) it was stated (ref 3) that a term of the form $F_E(v,T)$ could make an anisotropic contribution to the stress tensor when the stretch ratios are unequal. This is only correct for the form of the stress tensor referred to the original area. For the usual stress tensor, referred to the present area, the contribution is hydrostatic.
(16) Boggs, F. W. *J. Chem. Phys.* **1952**, *20*, 632.
(17) Eichinger, B. E. *Macromolecules* **1981**, *14*, 1071.
(18) DiMarzio, E. A. *J. Chem. Phys.* **1962**, *36*, 1563.
(19) Jackson, J. L.; Shen, M. C.; McQuarrie, D. A. *J. Chem. Phys.* **1966**, *44*, 2388.
(20) Gaylord, R. J. *Polym. Eng. Sci.* **1979**, *19*, 263.
(21) See, for example: Weiner, J. H. *Statistical Mechanics of Elasticity*; Wiley: New York, 1983; pp 234–237.
(22) Gao, J.; Weiner, J. H. *Macromolecules* **1987**, *20*, 142.
(23) Treloar, L. R. G. *The Physics of Rubber Elasticity*, 3rd ed.; Clarendon: Oxford, 1975; pp 113–116.
(24) Chandler, D.; Weeks, J. D.; Andersen, H. C. *Science (Washington, D.C.)* **1983**, *220*, 787.
(25) Flory, P. J. *Statistical Mechanics of Chain Molecules*; Interscience: New York, 1969; p 315.
(26) Weiner, J. H.; Berman, D. H. *J. Chem. Phys.* **1985**, *82*, 548.
(27) Berman, D.; Weiner, J. H. *J. Chem. Phys.* **1985**, *83*, 1311.
(28) Lecture notes by A. Rahman, Aug 2, 1985, unpublished results. Sullivan et al. (Sullivan, F.; Mountain, R. D.; O'Connell, J. *J. Comp. Phy.* **1985**, *61*, 138) provided useful guides to vectorizable algorithms for molecular dynamics calculations.

Ultimate Elastic Modulus and Melting Behavior of Poly(oxymethylene)

J. Runt,* R. F. Wagner, and M. Zimmer

Polymer Science Program, Department of Materials Science and Engineering, The Pennsylvania State University, University Park, Pennsylvania 16802.
Received February 9, 1987

ABSTRACT: The ultimate crystalline modulus of poly(oxymethylene) was estimated by using the Raman longitudinal acoustic mode and small-angle X-ray scattering. In this paper we emphasize the sensitivity of the calculated modulus to the values chosen for the thickness of the crystalline regions. Assuming that the uniform elastic rod model provides an adequate description of the LAM, we found E_c = 146 GPa, in excellent agreement with the results of neutron-scattering experiments. We have also explored the melting behavior of the solution-crystallized materials used in this study. The estimated value of the fold surface free energy ($\doteq$88 ergs/cm^2) indicates a work of chain folding near 4 kcal/mol folds, a value in line with that found for other polyethers.

Introduction

Some 40 years ago, Mizushima and Shimanouchi[1] observed a band in the low-frequency Raman spectra of crystalline *n*-alkanes whose peak position varied inversely with the paraffin chain length. This band was assigned to a longitudinal accordion-like motion of the *n*-alkane chains and has been termed the longitudinal acoustic mode (LAM). Using an analogy with the case of a simple elastic rod, they found that the LAM peak frequency (ν) was related to the paraffin chain length (l) by

$$\nu = \frac{m}{2cl}\left(\frac{E}{\rho}\right)^{1/2} \quad (1)$$

where m is the mode order, c is the speed of light, and E and ρ the elastic modulus and density of the elastic rod.

Since this initial work, LAM's have been observed for a number of semicrystalline polymers.[2] In crystalline polymers, the accordion-like vibration is usually envisioned as being decoupled at the "interface" between the crystal core and fold surface and, as a consequence, l in eq 1 is taken as the crystalline thickness and E and ρ should correspond to E_c and ρ_c, the modulus and density of the crystalline core.

Since ρ_c is generally known and if the simple elastic rod model provides an adequate description of polymeric LAMs, measurement of l and ν can yield E_c directly. For the semicrystalline polymers studied thus far, the values of E_c determined by the LAM–uniform elastic rod approach agree quite well with those determined from neutron-scattering measurements.[3,4] However, a rather large discrepancy often exists between these values and those determined from X-ray crystal strain measurements. It appears that the primary assumption employed in the X-ray analysis (i.e., that the stress applied to the specimen is distributed homogeneously) is not a good approximation. This is the implication from the work of Brew et al.,[5] who examined the apparent crystal modulus of polyoxymethylene (POM) by the X-ray technique. The apparent modulus was found to vary from 44 GPa at room temperature to 105 GPa at −165 °C. The authors regard this latter value as a lower limit for the true E_c if at −165 °C the amorphous modulus is significantly less than E_c.[5]

In studies where ultimate crystalline moduli have been derived from LAM experiment, melt-crystallized or annealed specimens have been frequently employed. The microstructure of these materials is generally quite complex and this complicates, for example, the assessment of

0024-9297/87/2220-2531$01.50/0